1202

# Preliminary crystallographic analysis and further characterization of a dodecaheme cytochrome *c* from *Desulfovibrio desulfuricans* ATCC 27774

ANA V. COELHO,[a,b] PEDRO M. MATIAS,[a] LARRY C. SIEKER,[a,c] J. MORAIS,[a] MARIA A. CARRONDO,[a,d]* JORGE LAMPREIA,[e] CRISTINA COSTA,[e] JOSÉ J. G. MOURA,[e] ISABEL MOURA[e] AND JEAN LE GALL[f] *at [a]Instituto de Tecnologia Química e Biológica, Apartado 127, 2780 Oeiras, Portugal, [b]Departamento de Química, Universidade de Évora, 7000 Évora, Portugal, [c]Department of Biological Structure, SM-20, University of Washington, Seattle, WA 98195, USA, [d]Instituto Superior Técnico, Av. Rovisco Pais, 1000 Lisboa, Portugal, [e]Departamento de Química e Centro de Química Fina e Biotecnologia, Faculdade de Ciências e Tecnologia, Universidade Nova de Lisboa, Quinta da Torre, 2825 Monte da Caparica, Portugal, and [f]Department of Biochemistry and Molecular Biology, University of Georgia, Athens, USA. E-mail: carrondo@itqb.unl.pt*

## Abstract

Dodecaheme cytochrome *c* has been purified from *Desulfovibrio* (*D.*) *desulfuricans* ATCC 27774 cells grown under both nitrate and sulfate-respiring conditions. Therefore, it is likely to play a role in the electron-transfer system of both respiratory chains. Its molecular mass (37 768 kDa) was determined by electrospray mass spectrometry. Its first 39 amino acids were sequenced and a motif was found between amino acids 32 and 37 that seems to exist in all the cytochromes of the $c_3$ type from sulfate-reducing bacteria sequenced at present. The midpoint redox potentials of this cytochrome were estimated to be −68, −120, −248 and −310 mV. Electron paramagnetic resonance spectroscopy of the oxidized cytochrome shows several low-spin components with a $g_{max}$ spreading from 3.254 to 2.983. Two crystalline forms were obtained by vapour diffusion from a solution containing 2% PEG 6000 and 0.25–0.75 $M$ acetate buffer pH = 5.5. Both crystals belong to monoclinic space groups: one is $P2_1$, with $a = 61.00$, $b = 106.19$, $c = 82.05$ Å, $\beta = 103.61°$, and the other is $C2$ with $a = 152.17$, $b = 98.45$, $c = 89.24$ Å, $\beta = 119.18°$. Density measurements of the $P2_1$ crystals suggest that there are two independent molecules in the asymmetric unit. Self-rotation function calculations indicate, in both crystal forms, the presence of a non-crystallographic axis perpendicular to the crystallographic twofold axis. This result and the calculated values for the volume per unit molecular weight of the $C2$ crystals suggest the presence of two or four molecules in the asymmetric unit.

## 1. Introduction

Heme proteins have an important role in many metabolic and biochemical pathways. They range from myoglobins and hemoglobins as oxygen storage and transport proteins through electron-transfer cytochromes, with one or more hemes, to a vast array of other proteins, some with enzymatic activity, containing only heme groups or hemes and other prosthetic groups. This rather ubiquitous use of the heme group in biochemical reactions suggests a great functional flexibility for this structure. In particular this is demonstrated by the cytochrome *c* family, which have midpoint redox potentials ranging from −400 to 500 mV (Pettigrew & Moore, 1987; Coutinho & Xavier, 1994).

A considerable amount of research has been invested in the determination of the crystal structures (Higuchi, Kusunoki, Matsuuna, Yasuoka & Kakudo, 1984; Matias, Frazão, Morais, Coll & Carrondo, 1993; Czjzek, Payan, Guerlesquin, Bruschi,

Haser, 1994; Morais *et al.*, 1995; Matias, Kissinger, Carrondo, Le Gall & Sieker, 1994; Matias *et al.*, 1996) and function studies (Coutinho & Xavier, 1994) of four-heme cytochromes $c_3$. The so-called cytochromes $c_3$ ($M_r = 26\,000$) (Bruschi, 1994) that have been found in *D. gigas* (Bruschi, Le Gall, Hatchikian & Dubourdieu, 1969) and in *Desulfomicrobium* (*Dm*) *baculatus* Norway 4 (Guerlesquin, Bovier-Lapierre & Bruschi, 1982) (formerly called *Desulfovibrio desulfuricans* Norway 4) are actually dimers and should be considered as a new family of tetraheme cytochromes analogous to cytochrome $c_3$. The X-ray crystal structure of the *Dm baculatus* protein is known (Czjzek, Payan & Haser, 1994) and a preliminary report on the crystallography of the *D. gigas* cytochrome has been published (Sieker, Jensen & Le Gall, 1986).

Besides the dimeric tetraheme cytochromes mentioned above the structures of cytochrome *c* containing more than four hemes, such as the hexaheme protein from *D. desulfuricans* which has nitrite reductase activity (Liu, Costa & Moura, 1994), as well as the hexadecaheme cytochrome which has been found in *D. vulgaris* strain Hildenborough (Higuchi, Inaka, Yasuoka & Yagi, 1987) and strain Miyazaki (Higuchi, Yagi & Voordouw, 1994) and in *D. gigas* (Chen, Pereira, Teixeira, Xavier & Le Gall, 1994) are still unknown. However, a preliminary report has been published on the crystallization of the *D. vulgaris* Hildenborough protein (Higuchi *et al.*, 1987). Herein we report preliminary crystallographic and structural studies on a dodecahemic cytochrome *c* ($M_r = 37\,768$), which has been isolated only from *D. desulfuricans* ATCC 27774 (Liu *et al.*, 1988). Very similar amounts of the protein were obtained from cells grown either in sulfate or nitrate-respiring conditions, indicating that this cytochrome is constitutively synthesized under both growing conditions and therefore likely to be an important electron carrier in both systems.

This cytochrome has been classified as one of the *c* type, since all 12 hemes appear to be covalently bound to the unique polypeptide chain. The number of cysteine residues, 26, determined from amino-acid analysis, is compatible with this classification. In addition, since no significant visible absorption was observed at 695 nm, it can be suggested that for the majority of the heme groups, the fifth and sixth coordination positions must be occupied by histidines and not by histidine-methionine residues.

The molecular mass was previously determined by sodium dodecyl sulfate polyacrylamide gel electrophoresis (SDS–PAGE) with and without removing the heme groups and confirmed by gel filtration as a monomer 27 774 (Liu *et al.*, 1988), giving a value of 40 800 Da.

The complete reduction of this cytochrome is possible after the addition of some crystals of sodium dithionite but not with ascorbate, which implies rather negative values for its midpoint redox potentials.

The determination of the three-dimensional structures of these high-heme content cytochromes is interesting as it will allow the analysis of possible interactions with redox partners, and will also expand our knowledge on the inter- and intraheme electron transfer of multihemic cytochromes.

## 2. Methods

### 2.1. Protein purification and crystallization

Cells were grown and the dodecahemic cytochrome purified following the protocol previously described (Liu *et al.*, 1988). The purity of the protein solution was checked by SDS–PAGE. In order to concentrate the protein solution to 10 mg ml$^{-1}$, the necessary final concentration for the crystallization procedure, it is necessary to decrease the ionic strength of the solution. As the protein seems to behave differently with time an additional step of gel-filtration chromatography with Superdex-75 was carried out when the crystallization did not produce crystals as good as those obtained from a fresh solution.

Crystallization conditions were screened using the hanging-drop vapour-diffusion method, but larger crystals could only be grown using the sitting-drop technique. The composition of the crystallization solution is: polyethylene glycol 6000, 2–10%(*w*/*v*), 0.25–0.75 *M* sodium acetate buffer, pH 5.5. Each drop was prepared by mixing 10 µl of the protein solution with the same amount of the crystallization solution on a polystyrene microbridge (DROP, Devis Realization Outillage Precision, Grenoble), and was equilibrated by vapour diffusion against 700 µl of the solution contained in the reservoir of a Linbro tissue-culture plate. The well was covered with a glass coverslip and sealed with silicone grease. The crystallization assays gave better results at 293 K.

### 2.2. Protein characterization

The molecular mass of the multiheme cytochrome was determined on a VG Bio-Q triple quadrupole mass spectrometer (Fisions Instruments, Altrincham, UK). The sample (10 ml containing 100 pmol of protein) was dissolved in acetonitrile/water/formic acid (50:49:1) and introduced in the electrospray mass spectrometer at a flow rate of 6 ml min$^{-1}$. The capillary voltage was set at 3.50 kV and the cone voltage was 5 V. Scans ranging from 600 to 1500 Da were accumulated during two minutes at a scan time of 9 s. The mass spectrometer was calibrated using horse myoglobin.

The N-terminal sequence was determined by the method of Edman & Begg (1967) using an Applied Biosystem sequencer model 470A.

The determined N-terminal sequence was aligned against several other cytochromes of the $c_3$ type. The overall alignment was obtained considering the known three-dimensional data for the sequences (Fig. 1) as performed by Palma *et al.* (1994). The other sequences were then aligned in accordance with this pattern. The open boxed region indicates an area of great structural flexibility in those four cytochromes of known three-dimensional structure, where this region corresponds to loops of different sizes; these were omitted from the alignment algorithm. The insertions shown are in arbitrary positions.

Analytical thin-layer electrofocusing in polyacrylamide gel was used to estimate the isoelectric point and purity of the cytochrome on a LKB Multiphor apparatus (Vesterberg, 1972). A pH gradient between 2.5 and 8.0 was achieved using ampholines.

### 2.3. Redox titration

Redox titration was performed on the multiheme cytochrome in 100 m*M* Tris–HCl, pH 7.6, in the presence of redox mediators (10 m*M* each), as previously described for nonheme iron protein titrations (Moura, Xavier, Cammack, Bruschi & Le Gall, 1978), under anaerobic conditions in an optical redox cell
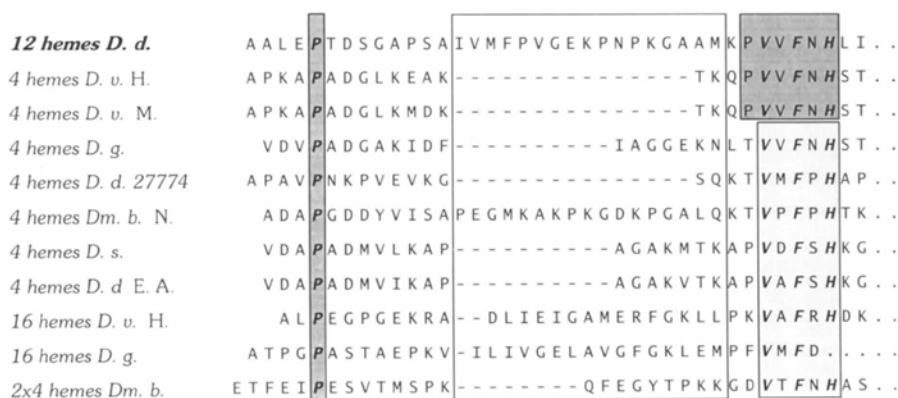


Fig. 1. The alignment of the N-terminal portions of several cytochromes. In grey the similarity areas. In bold and italic, the conserved amino acids. The sequences of the four-heme cytochromes isolated from *D. vulgaris* Miyazaki, *D. gigas*, *D. desulfuricans* 27774 and *Dm. baculatus* Norway 4 were aligned based on their three-dimensional structures. The open-boxed region indicates an area of great flexibility not submitted to any kind of alignment algorithm. **12 hemes D. d.**, dodecaheme cytochrome from *D. desulfuricans* ATCC 27774; 4 hemes D. v. H., cytochrome $c_3$ from *D. vulgaris* Hildenborough; 4 hemes D. v. M., cytochrome $c_3$ from *D. vulgaris* Miyazaki; 4 hemes D. g., cytochrome $c_3$ from *D. gigas*; 4 hemes D. d. 27774, cytochrome $c_3$ from *D. desulfuricans* ATCC 27774; 4 hemes Dm. b. N., cytochrome $c_3$ from *Dm. baculatus* Norway 4; 4 hemes D. s., cytochrome $c_3$ from *D. salexigens*; 4 hemes D. d. E. A., cytochrome $c_3$ from *D. desulfuricans* El Agheila; 16 hemes D. v. H., high-molecular-weight cytochrome (Hmc) from *D. vulgaris* Hildenborough; 16 hemes D. g., high-molecular-weight cytochrome (Hmc) from *D. gigas*; 2 × 4 hemes Dm. b. N., dimeric cytochrome $c_3$ from *Dm. baculatus* Norway 4.

by a method slightly modified from the design of Dutton (1971). The cell, containing a volume of 3 ml, was kept under a continuous stream of argon gas. The potential was varied by the injection of appropriate amounts of deaerated 3 m$M$ sodium dithionite and measured with a Crison Micro pH2002 digital pH meter. Optical spectra were recorded throughout the titration on a UV/Vis Shimadzu UV-265 spectrophotometer.

### 2.4. EPR spectroscopy

Electron paramagnetic resonance (EPR) spectroscopy was performed on a Bruker ER 200tt spectrometer equipped with an Oxford Instruments ESR910 continuous-flow helium cryostat.

### 2.5. Crystallographic diffraction data collection and evaluation

The diffraction data were collected using an Enraf–Nonius FAST area detector diffractometer coupled to an Enraf–Nonius FR-571 rotating-anode generator, operated at its maximum power (45 kV 99 mA) and equipped with a graphite mono-chromator, using Cu $K\alpha$ ($\lambda = 1.5418$ Å) radiation collimated at 0.3 mm. The parameters used for data collection on both crystal forms are summarized in Table 1. In order to optimize the statistical quality of the data, crystals had their twofold crystallographic axis almost aligned with the $\omega$ axis.

Preliminary unit-cell dimensions and space group were obtained by an autoindexing procedure. In order to obtain unique data sets as complete as possible, separate measure-ments were carried out varying the orientation of the crystal relative to the beam. Intensity-data measurements and indexing of reflections were made using the program MADNES (Pflugrath & Messerschmidt, 1989) after profile fitting by the average spot-profile algorithm. The intensity data were converted to the CCP4 package (Collaborative Computational Project, Number 4, 1994), the four separate data sets were scaled and merged together, and finally, the intensities were truncated to structure-factor amplitudes.

The diffraction symmetry pattern of the $P2_1$ crystals was recorded by precession photographs obtained from the same source operated at 40 kV, 75 mA and an Enraf–Nonius FR-504 precession camera. The X-ray radiation was filtered with a nickel filter and collimated with a 0.3 mm collimator. The two zero-layer precession photographs were separated by 90 about the spindle axis, one precessing around the $b$ axis and another precessing around the $c$ axis, with a precession angle, $\mu$, of 10 , in each case. The crystal was exposed for about 15 h, the crystal-to-film distance was 100 mm and a screen with radius of 1 cm was used at a distance from the crystal equal to 56.8 mm.

### 2.6. Crystal density measurements

The number of protein molecules per asymmetric unit in the $P2_1$ crystal form was calculated from measurements of the crystal density. The crystal density determination used a Ficoll (Pharmacia) gradient calibrated with glass spheres of known density following the procedure described by Bode & Schimer (1985).

### 2.7. Self-rotation function calculation

The presence of a non-crystallographic symmetry axis relating the molecules in the asymmetric unit was detected by the examination of the self-rotation function, performed using two different programs and spherical polar coordinates ($\omega, \varphi, \kappa$): PROTEIN (Steigemann, 1974) and POLARRFN (Collaborative Computational Project, Number 4, 1994). The solutions

Table 1. *Parameters used for data collection on each crystal form*

| Data-collection parameters | Crystal forms | |
|---|---|---|
| | C2 | $P2_1$ |
| Crystal-to-detector distance (mm) | 60 | 75 |
| Swing angle between the detector and the beam ( ) | 0 | 15 |
| Rotation scans around $\omega$ ( ) | 0.1 | 0.15 |
| Exposure time per frame (s) | 45 | 60 |

obtained were confirmed for different Patterson radii and resolution ranges. The absence of a non-crystallographic binary axis parallel to the twofold crystallographic axis was confirmed by the analysis of the Patterson function, calculated with FFT (Collaborative Computational Project, Number 4, 1994).

## 3. Results and discussion

### 3.1. Biochemical characterization and N-terminal sequence comparisons

The purified dodecaheme cytochrome $c$ shows a single band on 12.5% SDS–PAGE gel confirming its purity. The molecular mass previously determined by SDS ($M_r = 40\,800$) was now redetermined by electrospray mass spectrometry giving the value 37 768 Da. The isoelectric point of the cytochrome was found to be 5.21.

The first 39 N-terminal amino acids of the dodecaheme cytochrome $c$ were sequenced and compared with several four-heme $c$-type cytochromes from sulfate-reducing bacteria namely the cytochrome $c_3$ from D. vulgaris Hildenborough, D. vulgaris Miyazaki, D. gigas, D. desulfuricans ATCC 27774, Dm baculatus Norway 4, D. salexigens and D. desulfuricans El Agheila, and two hexadecaheme $c$-type cytochromes from D. vulgaris Hildenborough and D. gigas, and the dimeric tetraheme $c$-type cytochromes from Dm baculatus Norway 4. All the sequences were extracted from the Swiss-Prot 31 Database, April 1995 (Bairoch & Boeckmann, 1991) using the PC-GENE 6.85 software package (Intelligenetics, Inc., 1992).

This comparison showed an extremely conserved pattern – VXFXH – immediately before the first heme-binding motif as well as an initial proline residue that is conserved. This similarity is even higher between the dodecaheme cytochrome and the two cytochromes $c_3$ from D. vulgaris Hildenborough and Miyazaki in which the pattern is fully conserved and becomes PVVFNH (Fig. 1). The position of this phenylalanine in the three-dimensional structures suggests a functional importance for this residue in the electron-transfer process (Moore & Pettigrew, 1990). Another interesting conclusion resulting from these comparisons is that the Dm baculatus Norway 4 dimeric cytochrome N terminal is different from all others, including the D. desulfuricans 12-heme protein. Indeed, all these cytochromes, except the dimeric one, possess an N-terminal sequence which is compatible with the presence of a signal peptidase cleavage site as defined by Le Gall & Peck (1987). There is no indication concerning the localization of the Dm baculatus dimeric cytochrome. However, the analogous protein from D. gigas has always been found in the cytoplasmic fractions of the cell extracts (Le Gall, Payne, Chen, Liu & Xavier, 1994): the N-terminal sequence of these cytochromes could be very significant as far as their localization and functions are concerned. The resemblance between the N terminals of the hexadecaheme cytochromes from D. vulgaris

and *D. gigas* and the dodecaheme protein in *D. desulfuricans* is also interesting. Although no high-spin heme has been found in the latter, in contrast to what is found in 16-heme cytochromes (see EPR results below) and that high yields of the protein are always obtained whatever growth conditions are used, the possibility of the 12-heme being a degradation product of a yet undetected 16-heme cytochrome cannot be discarded entirely.

### 3.2. *Redox potentials*

The reduction potentials for the dodecaheme cytochrome *c* at pH 7.6 were estimated measuring visible absorbance changes at 553 nm as a function of the solution redox potential (Fig. 2). The experimental curves were adjusted with four Nernst equations, with redox potential of −68, −120, −248 and −310 mV, in a ratio of 2:1:5:4.

### 3.3. *EPR spectroscopy*

The EPR spectroscopy of the oxidized dodecaheme cytochrome (Fig. 3) shows several low-spin components with $g_{max}$ values ranging from 3.254 to 2.983. A $g_{med}$ of 2.250 and a $g_{min}$ of 1.515 are also observed and correspond to the $g_{max}$ 2.983. The spectrum resolution does not allow the deconvolution of

the 2.983 $g_{max}$ region into several low-spin components. However, it is possible to identify in the spectrum that some of the hemes have a $g_{max}$ around 3.254, a value closer to a more axial ligand field which for a bis-histidine ligation indicates a non-coplanarity of the imidazole planes.

### 3.4. *Crystallization of dodecaheme cytochrome c*

Crystals of the two forms, rectangular prisms and long needles, were obtained in each drop, in different proportions, depending on the concentration of acetate buffer used. With a lower concentration of buffer more needle-shaped crystals were formed, their number decreased gradually until the 0.75 *M* buffer concentration was reached. At the higher buffer concentration used, 0.75 *M*, only rectangular prisms were obtained. Usually a cluster of long needles grows from the same nucleus. In some drops it was possible to obtain large enough needles (0.6 × 0.2 × 0.15 mm) to record their diffraction pattern. This crystal form appears before the rectangular prisms and reaches its maximum size faster. The rectangular prisms took about 2–6 d to appear and 2–3 weeks to reach their maximum size (1.0 × 0.6 × 0.6 mm). The morphology of both crystal forms is illustrated in Figs. 4(a) and 4(b).
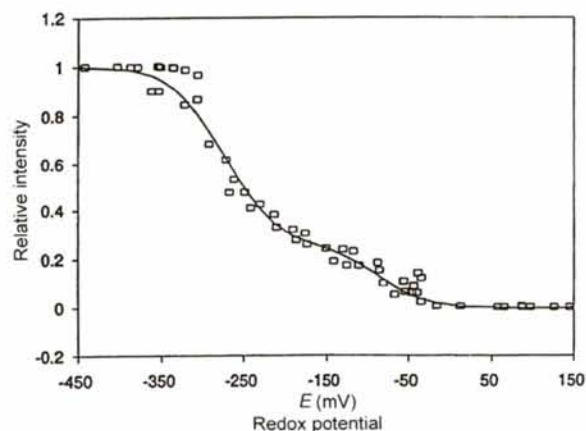


Fig. 2. Visible redox titration curve of the dodecaheme cytochrome. The curve is the result of the fitting of four independent Nernst equations using $E_1 = -68$, $E_2 = -120$, $E_3 = -248$, $E_4 = -310$ mV. Absorbance was measured at 553 nm.
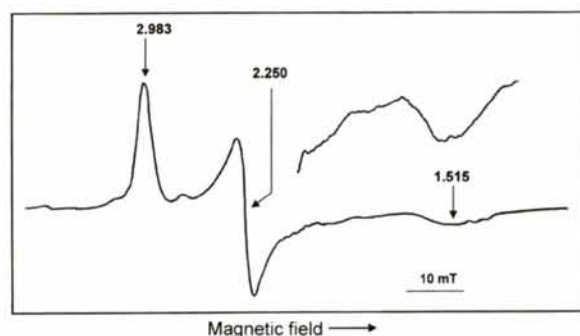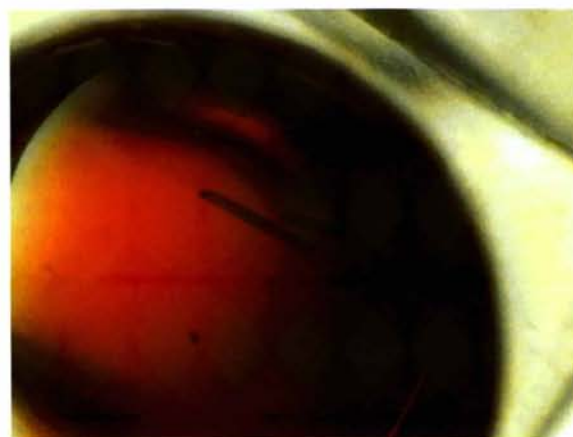


(a)



Fig. 3. EPR spectrum of the oxidized dodecaheme cytochrome. $T = 12$ K; microwave power = 0.2 mW; modulation amplitude = 1 mT; frequency = 9.525 GHz.
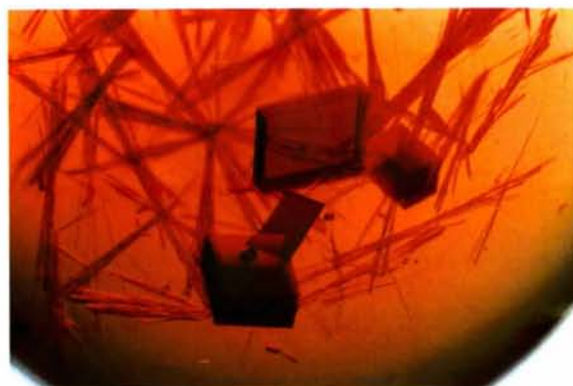
(b)

Fig. 4. Crystals of dodecaheme cytochrome *c* from *D. desulfuricans* ATCC 27774: (a) *C*2 needle crystals, (b) *P*2₁ rectangular prims. Approximate length of the largest crystal with rectangular prism shape is 1.0 mm.

### 3.5. Characterization of the crystals, X-ray data collection and evaluation

The rectangular prisms belong to the monoclinic system and from the systematic absences it was possible to determine the space group as $P2_1$. This space group is confirmed by the precession photographs (Fig. 5), which show the existence of a binary symmetry axis visible in the $h0l$ plane and the systematic absences ($k = 2n + 1$) along the $b^*$ axis on $hk0$ plane.
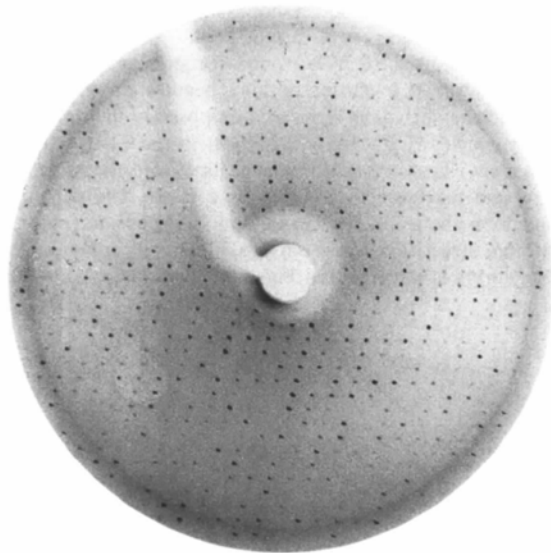
(a)
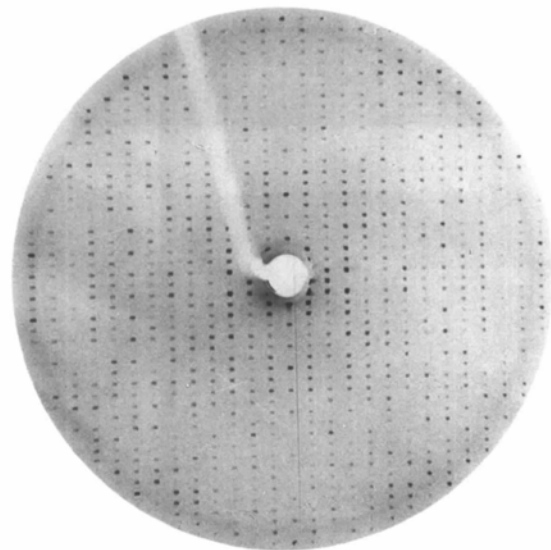
(b)

Fig. 5. Precession photographs of $P2_1$ form crystals of dodecaheme cytochrome $c$ from *D. desulfuricans* ATCC 27774: (a) for $h0l$ plane and (b) for $hk0$ plane, showing the binary axis symmetry and the systematic absences due to the space-group symmetry $P2_1$.

Table 2. *Statistical analysis results of the diffraction data sets collected for each crystal form*

| | Crystal forms | |
| --- | --- | --- |
| Parameters | C2 | $P2_1$ |
| No. of observations measured | 34898 | 69988 |
| No. of unique reflections | 9157 | 22512 |
| Resolution range (Å) | 100.0–4.0 | 38.0–2.9 |
| Completeness (%) | 93.1 | 99.5 |
| Completeness in last resolution shell (Å) | 75.4 (4.10–4.00 Å) | 96.4 (2.98–2.90 Å) |
| Average $I/\sigma(I)$ | 6.7 | 5.3 |
| $R_{\mathrm{merge}}(I)$ (%) | 10.4 | 11.1 |
| $R_{\mathrm{merge}}(I)$ in last resolution shell (%) | 26.6 (4.10–4.00 Å) | 31.4 (2.98–2.90 Å) |
| Cell dimensions (Å, °) | $a = 152.17$, $b = 98.45$, $c = 89.24$, $\beta = 119.18$ | $a = 61.00$, $b = 106.19$, $c = 82.05$, $\beta = 103.61$ |
| $V_m$ (Å$^3$ Da$^{-1}$) (molecules per asymmetric unit) | 3.85 (2) 1.93 (4) | 3.42 (2) 2.28 (3) |

Diffraction data were processed following the procedure described above in *Materials and methods*. Table 2 shows the results for the statistical analysis of the diffraction data collected for each crystal form.

As two values are possible for the volume per unit molecular weight, $V_m$, of the $P2_1$ crystal form [the limits found by Matthews on a study using several protein crystals are 1.7 to 3.5 Å$^3$ Da$^{-1}$ (Matthews, 1968)], the determination of crystal density was used to decide between the two possibilities. The measured value of 1.136 g ml$^{-1}$ for the crystal density indicates that there are two molecules per asymmetric unit ($V_m = 3.42$ Å$^3$ Da$^{-1}$) with a solvent content of 64.0%. The self-rotation function calculation confirmed this result, since the presence of a non-crystallographic twofold axis perpendicular to the crystallographic twofold ($b$) axis (Fig. 6$a$) was found, with a height of 2.4$\sigma$ above the background. The combination of these two axes gives rise to a third axis perpendicular to the other two. This result was obtained with the two programs used for the self-rotation function calculations, carried out with different resolution ranges (10–3, 10–3.5 Å) and different Patterson radii (20–5, 15–5 Å). An independent calculation using the Patterson function confirms that the pseudo-axis relating the two molecules in the asymmetric unit is not parallel to the twofold screw (crystallographic $b$) axis.

For the C2 crystals the calculation of the self-rotation function suggests the same kind of orientation for the twofold pseudo-axis relating the two or four molecules in the asymmetric unit. The same pattern was obtained for the stereogram using different resolution ranges (20–4, 20–4.5 Å) and different Patterson radii (20–5, 15–5 Å), where two peaks with a height 2.4$\sigma$ over the background could be identified (Fig. 6$b$). The possible existence of three molecules in the asymmetric unit of this crystal form (following the determined values for the volume per molecular weight) was excluded after the analysis of this calculation.

Because of the fragility of the needle-shaped crystals it was not possible to determine their density in order to decide the real content in the asymmetric unit. Thus, it may be composed of two molecules giving a $V_m$ value of the crystal slightly higher than usual (3.85 Å$^3$ Da$^{-1}$), with a solvent content (68%) close to

the value determined for $P2_1$ crystals, or there are four molecules in the asymmetric unit, corresponding to a $V_m$ value (1.93 Å$^3$ Da$^{-1}$) included in the Matthews range but a solvent content (36.1%) almost half of that found for the $P2_1$ crystals.



(a)



(b)

Fig. 6. Self-rotation function plots for dodecaheme cytochrome $c$: (a) crystal form $P2_1$ in resolution range $3 \le d \le 10$ Å with integration range $5 \le R \le 20$ Å, and (b) crystal form $C2$ in resolution range $4 \le d \le 20$ Å with integration range $5 \le R \le 20$ Å. Peaks in the section shown ($\kappa = 180°$) give the orientation of the twofold axis in the crystal structure. The maximum value was normalized to 100 and the contours drawn at 5 unit intervals beginning at 40. The central peak is the crystallographic twofold and the two smaller features (height 70) correspond to the two non-crystallographic twofold rotation axes.

This hypothesis is, however, less probable since the $C2$ crystals are very fragile and diffracted only to 4.0 Å, therefore indicating a higher solvent content than that of the $P2_1$ crystals, and thus two molecules per asymmetric unit.

In order to determine the phases to calculate electron-density maps several experiments involving the preparation of heavy-atom derivatives were made, but the difference Patterson maps were difficult to interpret. To overcome this problem the multiple-wavelength anomalous dispersion method of phase determination is being considered. A cytochrome molecule with 12 Fe atoms per molecule is a suitable candidate for MAD data-collection experiments. Work in this direction is currently under way.

*Note added in proof*: a full description of the octaheme cytochrome $c_3$ ($M_r$ 26 000) from *Dm baculatus* has recently been published (Czjzek, Guerlesquin, Bruschi & Haser, 1996).

### References

Bairoch, A. & Boeckmann, B. (1991). *Nucleic Acids Res.* **19**, 2247–2249.

Bode, W. & Schirner, T. (1985). *Hoppe-Seyler's Biol. Chem.* **366**, 287–295.

Bruschi, M. (1994). *Methods Enzymol.* **243**, 140–155.

Bruschi, M., Le Gall, J., Hatchikian, C. E. & Dubourdieu, M. (1969). *Bull. Soc. Franç. Physiol. Végét.* **15**, 381–390.

Chen, L., Pereira, M. M., Teixeira, M., Xavier, A. V. & Le Gall, J. (1994). *FEBS Lett.* **347**, 295–299.

Collaborative Computational Project, Number 4. (1994). *Acta Cryst.* D**50**, 760–763.

Coutinho, I. B. & Xavier, A.V. (1994). *Methods Enzymol.* **243**, 119–140.

Czjzek, M., Guerlesquin, F., Bruschi, M. & Haser, R. (1996). *Structure*, **4**, 395–404.

Czjzek, M., Payan, F., Guerlesquin, F., Bruschi, M., Haser, R. (1994). *J. Mol. Biol.* **243**, 653–667.

Czjzek, M., Payan, F. & Haser, R. (1994). *Biochimie*, **76**, 546–553.

Dutton, L. D. (1971). *Biochem. Biophys. Acta*, **226**, 63–80.

Edman, P. & Begg, G. (1967). *Eur. J. Biochem.* **1**, 80–91.

Guerlesquin, F., Bovier-Lapierre, G. & Bruschi, M. (1982). *Biochem. Biophys. Res. Commun.* **105**, 530–538.

Higuchi, Y., Inaka, K., Yasuoka, N. & Yagi, T. (1987). *Biochem. Biophys. Acta*, **911**, 341–348.

Higuchi, Y., Kusunoki, M., Matsuuna, Y., Yasuoka, N. & Kakudo, M. (1984). *J. Mol. Biol.* **172**, 109–130.

Higuchi, Y., Yagi, T. & Voordouw, G. (1994). *Methods Enzymol.* **243**, 155–165.

Intelligenetics, Inc. (1992). *PC-GENE* 6.85 software package. Intelligenetics, Inc., 700 East El Camino Real, Mountain View, California 94040, USA.

Le Gall, J., Payne, W. J., Chen, L., Liu, M. Y. & Xavier, A. V. (1994). *Biochimie*, **76**, 655–665.

Le Gall, J. & Peck, H. D. Jr (1987). *FEMS Microbiol. Rev.* **46**, 35–40.

Liu, M.-C., Costa, C., Coutinho, I. B., Moura, J. J. G., Moura, I., Xavier, A. V. & Le Gall, J. (1988). *J. Bacteriol.* **170**, 5545–5551.
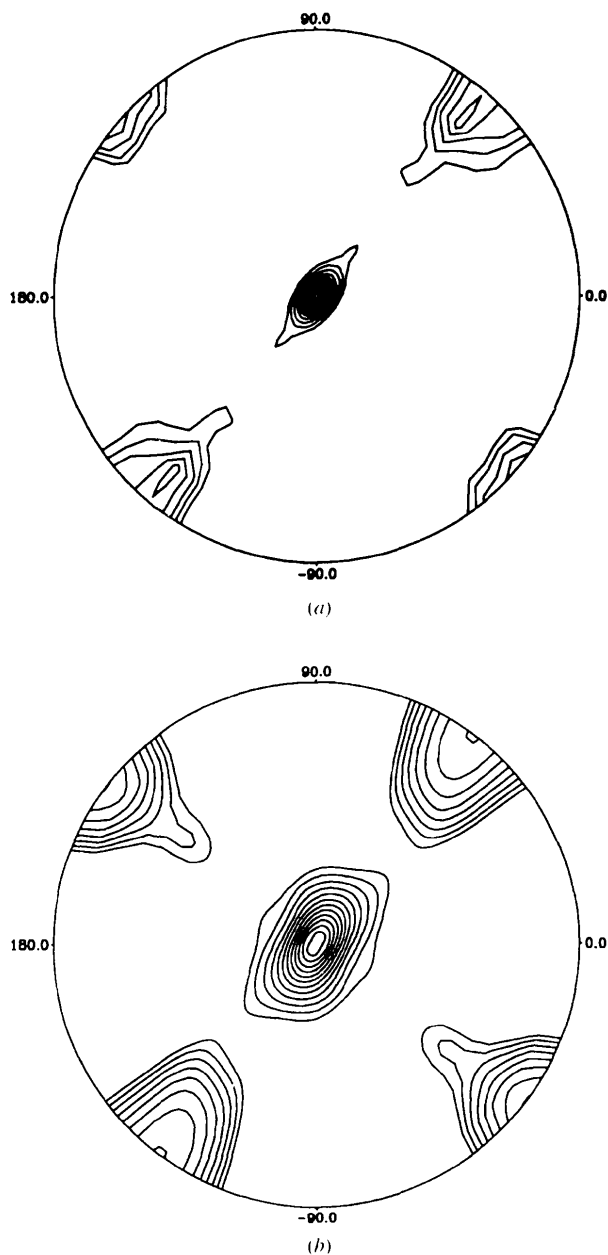
Liu, M.-C., Costa, C. & Moura, I. (1994). *Methods Enzymol.* **243**, 303–319.

Matias, P. M., Frazão, C., Morais, J., Coll, M. & Carrondo, M. A. (1993). *J. Mol. Biol.* **234**, 680–699.

Matias, P. M., Kissinger, C., Carrondo, M. A., Le Gall, J. & Sieker, L. (1994). Am. Crystallogr. Assoc. Meet. Inforum, Atlanta, Georgia, USA.

Matias, P. M., Morais, J., Coelho, R., Carrondo, M. A., Wilson, K., Dauter, Z. & Sieker, L. (1966). *Protein Sci.* **5**, 1342–1354.

Matthews, B. W. (1968). *J. Mol. Biol.* **33**, 491 497.

Moore, G. R. & Pettigrew, G. W. (1990). *Cytochromes c – Evolutionary, Structural and Physicochemical Aspects*, pp. 241–249. *Springer Series in Molecular Biology*. Berlin: Springer-Verlag.

Morais, J., Palma, P. N., Frazão, C., Caldeira, J., Moura, I., Le Gall, J., Moura, J. J. G. & Carrondo, M. A. (1995). *Biochemistry*, **34**, 12830–12841.

Moura, I., Xavier, A. V., Cammack, R., Bruschi, M. & Le Gall, J. (1978). *Biochem. Biophys. Acta*, **533**, 156–162.

Palma, P. N., Moura, I., Le Gall, J., Van Beeumen, J., Wampler, J. E. & Moura, J. J. G. (1994). *Biochemistry*, **33**, 6394–6407.

Pettigrew, G. W. & Moore, G. R. (1987). *Cytochromes c – Biological Aspects*, pp. 1–28. *Springer Series in Molecular Biology*. Berlin: Springer-Verlag.

Pflugrath, J. W. & Messerschmidt, A. (1989). *MADNES*, Munich Area Detector New EEC System. Cold Spring Harbor Laboratory, Cold Spring Habor, NY 11724 USA, and Max-Planck Institut für Biochemie, Martinsried, Germany.

Sieker, L. C., Jensen, L. H. & Le Gall J. (1986). *FEBS Lett.* **209**, 261–264.

Steigemann, W. (1974). PhD thesis, Technische Universität, München, Germany.

Vesterberg, O. (1972). *Biochem. Biophys. Acta*, **257**, 11–19.